Biochimica et Biophysica Acta, 634 (1981) 289—308

BBA 47999

THE pH DEPENDENCE OF PHOTOSENSORY RESPONSES IN *STENTOR COERULEUS* AND MODEL SYSTEM

EDWARD B. WALKER, MINJOONG YOON and PILL-SOON SONG *

Department of Chemistry, Texas Tech University, Lubbock, TX 79409 (U.S.A.)

(Received August 7th, 1980)

Key words: Photophobic response; Photoreceptor; Sensory transduction; Phototaxis; Membrane potential; Proton gradient; Fluorescence quenching; (Stentor coeruleus)

Summary

1. Live *Stentor coeruleus* exhibits a substantially red-shifted fluorescence maximum, corresponding to the anionic species of the photoreceptor chromophore. No change was observed in either the absorption or fluorescence excitation spectrum, indicating an efficient deprotonation of the photoreceptor pigment upon excitation by light.

2. Changes in external pH exhibit a dramatic effect on the photosensory response of *Stentor*. Phototaxis is specifically inhibited at pH < 6, with loss of photosensory perception which is restored when the pH is returned to pH > 6.

3. Fluorescence changes of 9-aminoacridine in suspensions of live *Stentor* indicate the generation of a pH gradient upon irradiation with light. Both pH gradient and phototaxis were inhibited by the addition of nigericin and *p*-trifluoromethoxy carbonyl cyanide phenylhydrazone (FCCP).

4. Incorporation of the *Stentor* photoreceptor protein into artificial liposomes demonstrates the ability of the system to generate pH gradients across model membranes as monitored by the quenching of 9-aminoacridine fluorescence. The effect of external pH on net proton movement in the model system is strikingly similar to the pH dependent photomovement of the live *Stentor*, thus lending support for transient proton flux being an important mode of light signal processing for photosensory transduction.

Introduction

Stentor coeruleus responds to an increase in light intensity and change in light direction by stopping (ciliary reversal), turning and swimming away from the source of light [1,2]. These photoresponses (photophobic response and

* To whom correspondence should be addressed.
Abbreviations: DMPC, dimyristoyl phosphatidylcholine; DMSO, dimethylsulfoxide; FCCP, *p*-trifluoromethoxy carbonyl cyanide phenylhydrazone.

negative phototaxis) are mediated by a photoreceptor pigment which has an absorption maximum at 610 nm [3]. The pigment is enclosed in pigment granules, which are in ordered rows near the cilia. Each of the spherical granules is surrounded by a membrane and appears to be held tightly against the inside of the cytoplasmic membrane, near the surface of the organism [4—6].

A recent study in our laboratory has established the identity of the chromophore in the *Stentor* photoreceptor pigment (stentorin) as hypericin [3]. However, the pigment in *Stentor* is covalently bound to a protein complex. Based upon the lowering of the pK_a of one or more hydroxyl groups of the chromophore in the excited state, a mechanism for the primary photoprocess was proposed [3].

Wood [7] suggested that ciliary reversal of the *Stentor* organism was due to an intracellular photic receptor potential generated in the vacuoles. A similar photic potential was recorded in the cytoplasm by means of a KCl-microelectrode across the cell membrane of *Stentor* [1].

We initiated the study to ascertain whether or not such a membrane potential results directly or indirectly from light-induced proton release from the photoreceptors. We have also investigated the generation of a proton gradient by light in phospholipid liposomes and in the suspension of live *Stentor* as a function of pH. In order to determine the pH gradient, the fluorescent pH indicator, 9-aminoacridine was employed, since fluorescence quenching of 9-aminoacridine is an excellent probe to measure pH gradients developed across membranes [8].

Materials and Methods

Materials

Stentor coeruleus was grown as described previously [3]. Synthetic phospholipid, dimyristoyl L-α-phosphatidylcholine (DMPC) was obtained from Sigma Chemical Co. Its purity was checked by observing single spot on thin-layer chromatography coated with Silica Gel GFDC (Woelm) in the solvent mixture, $CHCl_3/MeOH/H_2O$ (65 : 25 : 4, v/v) [9]. Sepharose 4B-200, 9-aminoacridine, Trizma and phosphate buffers were also obtained from Sigma Chemical Co. 9-Aminoacridine was recrystallized three times from aqueous acetone in the presence of charcoal. Nigericin was obtained from the Eli Lilly Lab., and spectroquality acetone from Eastmann Organic Chemical Co. was used. Dimethylsulfoxide (DMSO), certified grade, was from Fisher Scientific.

Methods

Absorption, fluorescence and fluorescence lifetimes were measured as described previously [3]. Emission spectra of whole, living *Stentor* were measured in a triangular cuvette, as were highly concentrated samples to avoid internal filtering and scattering effects at high absorbances. Analysis of the fluorescence lifetimes was accomplished by utilization of an algorithm (Weber, G., personal communication).

Preparation of the *Stentor* photoreceptor complex was carried out by ammonium sulfate fractionation and differential centrifugation [3], yielding a distinct blue-green colored band on the isoelectric focussing column with an iso-

electric point of 5.1. Concentration of the photoreceptor complex was accomplished by means of membrane ultrafiltration in an Amicon Ultrafiltration cell, utilizing a Diaflo PM10 membrane. Concentration of the photoreceptor complex was monitored by absorbance at either 610 nm or at the excitation wavelength of 560 nm.

In order to quantitate the pH dependence of photoresponses in *Stentor* to an external light source, two different methods of analysis were used. The first method followed simultaneous determination of the rate of response and the total response of a population of *Stentor* to either white light or light of a desired wavelength. A large number of *Stentor*, approx. 100 to 1500 in 2.0 ml of growth medium, were placed in a $10 \times 0.5 \times 1$ cm gel-scanning cuvette (ultraviolet glass from Matheson Scientific) and allowed to equilibrate to an even population throughout the cuvette over a period of about 2 min in the dark. The light stimulus (fluence rate 28 W/m^2) from a Nicolas microscope illuminator was presented from a distance of eight inches away and two inches above the plane of the cuvette, through appropriate filters.

The responding *Stentor* swam away from the light toward the far end of the cuvette, where their accumulation was monitored by an infrared light beam (*Stentor* does not respond to wavelengths of light greater than 700 nm [1,7]). The infrared light source was a 40 W tungsten light bulb, filtered by an infrared-passing plastic filter. The filtered beam was delivered to the far end of the cuvette via a fiber optic bundle (Oriel Optics) of high transmission characteristics such that it traversed the cuvette perpendicular to the stimulating light. After passing through the solution of *Stentor*, the monitoring light was again filtered by an identical infrared-passing filter, before impinging on a cadmium sulfide photocell. Since the stimulating beam was always filtered by an infrared-absorbing filter (Oriel), very little if any scattered light reached the photocell.

The CdS photocell was chosen as the sensor, due to its sensitivity in the infrared region of the spectrum and its 'slow' response time, compared to a photomultiplier tube. The small size of the photocell is also an advantage in such an experimental device. A diffuser plate was also used in front of the photocell to help eliminate 'noise' in the signal, due to *Stentor* swimming randomly through the beam. As more *Stentor* swam away from the stimulating light into the infrared beam, less light reached the photocell, and a drop in the output voltage of the amplifier is recorded. The decrease in light reaching the photocell is a direct measure of the number of *Stentor* responding to the stimulating light.

The second method of quantitating the response involved a similar channel, which was cut into a plexiglass block. The channel was cut 9.0 mm deep, 6.2 mm wide and 75 mm long, and fitted on one end with a hinged lid. Four thin pieces of glass were inserted into the clear plexiglass lid, such that when the lid was closed the channel was divided into five sections, each measuring 15 mm in length. Each section represented 20% of the total volume of the channel. One end of the channel was covered with a quartz, non-birefringent plate. The light stimulus was presented through this plate directly into the suspension of *Stentor*, after passing through appropriate filters. After free swimming *Stentor* had responded to the light for a given amount of time, the lid was closed and

the plexiglass block containing the sectioned channel was placed under the stereomicroscope, where the number of *Stentor* in each compartment was counted. Each of the five channels was identified by a letter A through E, with A being the compartment furthest away from the light. For each experiment, at least five determinations were made with fresh *Stentor* for each experiment before a data point was recorded. Approximately 2 min were needed to completely randomize the *Stentor* in the dark before the light was turned on. A longer period than this resulted in *Stentor* attaching themselves to the wall or bottom of the channel, thus being not free to respond to the light. To insure reproducibility of light intensity, the entire apparatus was mounted on a plexiglass frame, and the removable channel was steadied by two pins on the main frame, which fit into the bottom of the channel block and held it firmly in place. Excellent reproducibility was obtained with this method over many weeks of experiments.

Although the apparatus is well suited to variable wavelengths of light, only wavelengths of 575 to 750 nm were used to stimulate the response (a combination of Corning CS2-63 colored glass filter and an infrared-absorbing heat filter). The light intensity was varied by using the three voltage settings on the Nicolas illuminator and a number of Oriel neutral density filters. The light intensity was measured with a Y.S.I. Kettering Radiometer, Model 65A.

In all experiments, where either pH was varied or a new substance was added to the medium, the solution of *Stentor* was allowed to equilibrate for 20 to 30 min before they were introduced into the channel for the experiment. *p*-Trifluoromethoxy carbonyl cyanide phenylhydrazone (FCCP) or nigerin was dissolved in DMSO at 1.0 mg/ml. Microliter aliquots of this solution were added to the *Stentor* suspension at pH 7.8. Equal amounts of DMSO without ionophores were added to controls, to ensure that the concentration of DMSO used to dissolve ionophores had no effect on the photoresponse.

Oxygen consumption experiments were carried out with a Y.S.I. Model 53 oxygen monitor on a 5.0 ml suspension of *Stentor* (7000 cells/ml). Oxygen concentration was set at appropriate levels by gently streaming a small flow of oxygen through the suspension of *Stentor* just prior to sealing them in the monitoring cell. Light stimulus was provided by the Nicolas Illuminator, which was filtered only for infrared light. The fluence rate of the incident white light was 30 W/m^2 at the surface of the cell. The solution was gently stirred by a magnetic stirbar in the bottom of the cell. The output from the oxygen monitor was plotted vs. time on an HP 7045A *X-Y*-recorder.

Preparation of Stentor photoreceptor-entrapped and imbedded liposomes. These preparations were performed by modification of Huang's method [10]. For the preparation of *Stentor* photoreceptor-entrapped DMPC liposome, a pigment protein preparation was evaporated to dryness in a rotary evaporator at room temperature under nitrogen at reduced pressure, and redissolved in 2 ml of 150—200 mM KCl solution or 10 mM phosphate buffer, which was adjusted to the desired pH by adding 0.01 M HCl. The aqueous suspension was sonicated in Bransonic 12 Sonifier for 1 h at room temperature. The thin film of DPMC lipid was prepared by evaporating chloroform solution of 10 mg of DMPC to dryness under reduced pressure at room temperature. The sonicated suspension of *Stentor* photoreceptor was centrifuged at $1000 \times g$ for 10 min at room

temperature, and then the supernatant was added to the DMPC thin film, followed by sonication in the Bransonic 12 Sonifier again for 90 min under nitrogen atmosphere at temperatures between 25 and 30°C. The resonicated dispersion was subjected to molecular sieve chromatography on Sepharose 4B column (2.5 × 20 cm) at room temperature. The absorption of column effluent at 280 nm was continuously recorded by using an ISCO Model UA-5 absorbance monitor.

For the preparation of photoreceptor-imbedded liposomes, acetone-extracted *Stentor* photoreceptor was dried, followed by redissolving in chloroform with 10 mg of DMPC lipid. This mixture was evaporated to dryness at room temperature under reduced pressure, yielding thin film. The thin film in 150—200 mM KCl solution was sonicated in the same manner as the resonication step above. All samples were handled under dim light or in darkness.

Determination of phase transition temperature of liposomes. Lipid phase transition temperatures of the photoreceptor-entrapped and -imbedded DMPC liposomes were determined by measuring the changes in fluorescence intensity of the pigment on the Perkin-Elmer Spectrofluorometer Model MPF-3, as a function of temperatures.

Determination of transmembrane pH gradient. Light-induced pH gradients across the membrane in the suspension of photoreceptor-entrapped liposome and live *Stentor* (2000 cells/2.5 ml) were determined by measuring the 9-aminoacridine fluorescence emission. Actinic light from an American Optics microscope lamp was passed through an infrared absorber and a Corning CS2-63 filter. Intensities of the actinic light were controlled by the combination of neutral density filters. The light intensity was measured with an Y.S.I. Kettering Radiometer.

The pH indicator probe, 9-aminoacridine (4 μM), was excited at 400 nm, and fluorescence quenching was monitored at 450 nm synchronously with the actinic beam.

The light-induced fluorescence quenching of 9-aminoacridine in photoreceptor-entrapped liposomes was converted to ΔpH by using the standard curve, which was obtained by measuring the quenching of 9-aminoacridine (4 μM) fluorescence as a function of ΔpH in the liposome without *Stentor* photoreceptor, as described in the literature [8,11].

Results

Stentor in normal growth medium at pH 7.8 responds to the light stimulus, swimming away from the light towards the far end of the channel. When monitored with the fiber-optic system, the response was complete in 2 min, with a well defined time-response curve as shown in Fig. 1. It was occasionally noted that if too many *Stentor* were in the cuvette and a large fraction swam to one end, a very dense population (cells/cm^3) was observed. This high concentration of *Stentor* was evidently not a favorable situation for some of the cells, since some began to swim away from the high concentration after the *Stentor* had congregated in the far end of the cuvette for one or two minutes. It is possible that the oxygen concentration was severely depleted in the immediate vicinity and the *Stentor* responded by swimming against the light gradient to an area of higher oxygen concentration. Oxygen consumption experiments indicated that

Stentor at this high population density quickly deplete the oxygen supply in their immediate vicinity.

When the pH of the medium was suddenly lowered more than 0.5 pH units, the shock caused initial cessation of the normal swimming behaviour and response to the light in a large majority of the *Stentor*. However, maximum response to the light is recovered in about 15 min, and for this reason a short incubation period of 20 to 30 min in the dark was used before each experiment.

Monitoring the movement away from the light was easily accomplished with the infrared-monitoring beam, since both time-dependent and total response could be monitored simultaneously. Since initial portions of the curve are good indications of the velocity of the responding *Stentor*, an increase in light intensity should yield a steeper curve if the swimming velocity increased with light intensity. However, under a wide range of light intensities, no change in swimming velocity was observed. Observation of the velocities of individual cells under the microscope was difficult to quantitate accurately due to three-dimensional movement and the different velocities of individual cells. It was noted, however, that under our experimental conditions, some individual cell velocities were in excess of 10 cm/min.

This method had some drawbacks, however. To reproduce the same response curve, it was critical to have exactly the same number of cells in the cuvette for each determination. Due to the large number of cells needed to efficiently block the infrared beam this was extremely difficult to do, and consumed large numbers of cells. Also, dead or damaged cells were not accounted for. It was

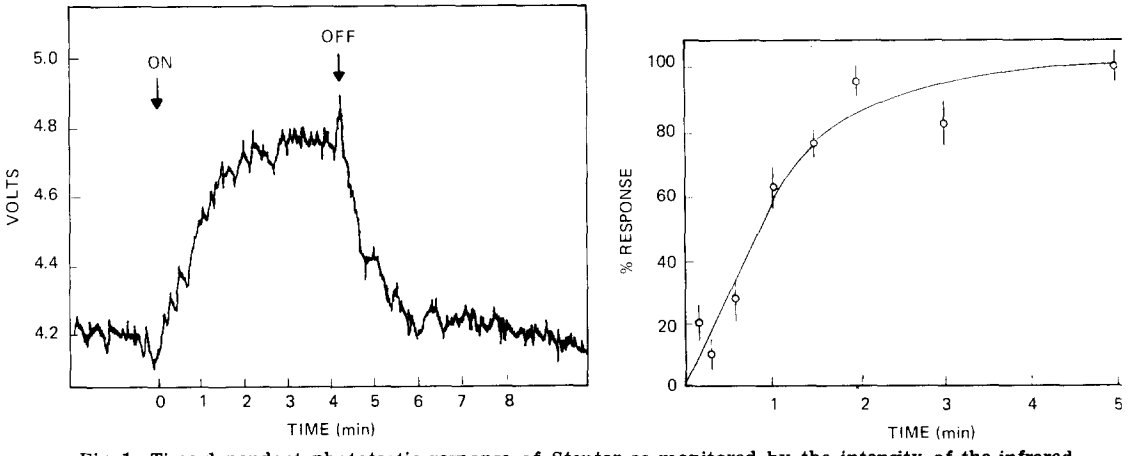

Fig. 1. Time-dependent phototactic response of *Stentor* as monitored by the intensity of the infrared beam reaching the CdS photocell (see Methods). *Stentor* responding to the actinic light swim into the infrared beam and decrease the amount of light reaching the photocell. The corresponding voltage drop is proportional to the number of cells responding to the light. The *y*-axis is inverted for comparison to the second method of analysis. The cuvette contained 1500 *Stentor* in 1.0 ml of growth medium at pH 7.8, and the actinic light intensity was 2.8 W/m^2 (575 nm $< \lambda <$ 750 nm).

Fig. 2. Time-dependent phototaxis as monitored by the actual number of *Stentor* swimming into compartment A of the channel described in Methods. % Response is defined in the text. Light intensity was 1.6 W/m^2 at the point where light entered the channel. The wavelength of the light stimulus was 575 to 750 nm.

therefore necessary to incorporate the second method of quantitation, the channel with compartments, where individual cells could be counted and examined. The few dead or damaged cells present were naturally not included in the populations of each compartment, while this was impossible with the other method. The time-dependent response of the *Stentor* was consistant with the previous method and the fraction of responding cells was the same. Fewer cells were used in the second method, averaging between 70 to 150 total cells per experiment, while the infrared beam required 1000 to 1500 cells. Better day-to-day reproducibility was noted for the second method also.

As seen in Fig. 2, the increase in the number of cells in compartment A as a function of time is virtually the same plot as obtained with the infrared-monitoring system. As is also seen, the population in A is directly correlated to the number of responding cells, as the number of cells in each of the other compartments decreases proportionally. Since the fraction of the total cells in compartment A is more sensitive as a method of measuring the response than a corresponding decrease in another compartment, the fraction of cells in A was calculated and plotted to analyze the response. At zero time the fraction of randomly distributed cells in compartment A equals 0.2. Therefore, when calculating the percent response, the cells in this compartment must be subtracted from the total cells at the end of each determination. Although these cells are responding, there is no way of measuring their response within the compartmental area. The percent response is therefore defined as

$$\% \text{ response} = \frac{(N_a/N_t - 0.2)}{(N_a^0/N_t^0 - 0.2)} \times 100$$

where N_a and N_t are the number of *Stentor* in compartment A and the total number of cells in the channel during the experiment, and the denominator is the control, where maximum response is observed. This was arbitrarily chosen to be the optimal growth medium conditions with pH 7.8 and was used as a control on each experiment. Normally the control fraction in A (N_a^0/N_t^0) was 0.75 to 0.80 after a 2-min light stimulus. The plotted curves appear identical, when either the Fraction in A or %response is used.

Very low thresholds of light perception were observed for *Stentors* at higher pH values. 10% response was noted as low as 0.1 W/m^2, while maximum response was reached at 0.8 to 1.0 W/m^2. Again, much higher light intensities did not result in faster swimming speeds, nor was the total responding fraction significantly increased.

On the other hand, much higher light intensities were needed to evoke a response from the *Stentor*, when pH was lowered below pH 6. The dose response curves at a number of pH values were determined, an example of which is shown in Fig. 3. First, a portion of the *Stentor* were subjected to light at pH 7.8 as is seen in the uppermost curve. The pH was then carefully lowered to 5.1; and, after a short incubation period, their dose-response curve determined. The particular curves show the response to a stimulus of 2.00 min. It must be stressed at this point that if the pH is lowered below 4.5 briefly, the vast majority of the *Stentor* will die. As a control, the pH is raised back to the original value of 7.8 after the completion of the experiment, so as to assure that the inhibition of the response was temporary. As is seen, restoration of the

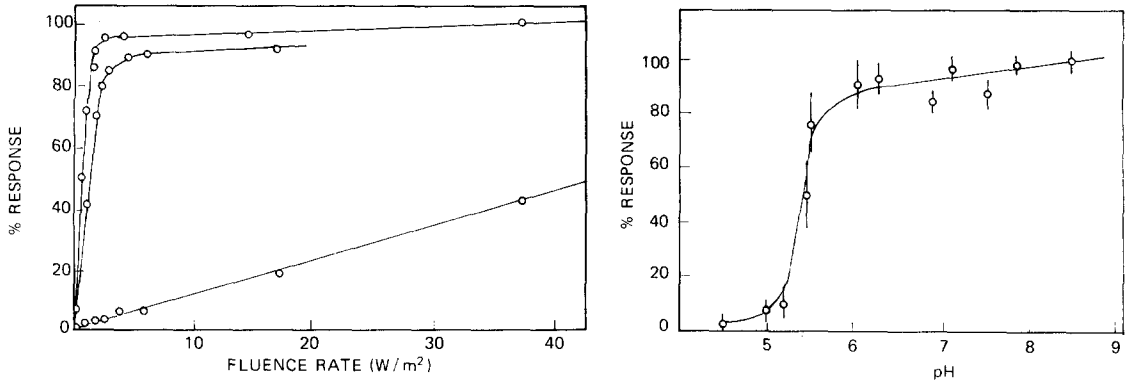

Fig. 3. A representative response curve of light intensity vs. % response at various pH values. Curve A is measured at pH 7.8. After pH was lowered to 5.1 with HCl, curve B was obtained. As a control, after 3 to 4 h at the lower pH value, the suspension was returned to pH 7.8 by the addition of NaOH. The restoration of phototaxis is seen in curve C.

Fig. 4. pH-dependent phototaxis of *Stentor*, constructed from a series of dose-response curves similar to Fig. 6, where % response was determined at 1.6 W/m^2. The confidence bars represent standard deviation on the results of at least five experiments at each pH value.

light response is virtually complete after as long as 3 or 4 h at the lower pH values.

From a series of dose-response curves, the profile of pH-dependent photoaxis was constructed in Fig. 4. A sharp decrease in response is seen at pH values lower than 6.0, with the decrease centered at pH 5.5. Less than 5% response is observed at pH values below 5.0. Longer periods of irradiation at lower pH values did not result in a larger number of responding cells.

This dependence on external pH prompted the investigation of proton ionophore effects on photomovement. One of the better known proton ionophores, FCCP, was used to probe the photoresponse. FCCP inhibited the response at micromolar concentrations as seen in Fig. 5, while the mortality rate was quite low (less than 5%) at total inhibition. DMSO at similar concentrations had no effect on the swimming rate or response to light.

Oxygen consumption by *Stentor* did not change if irradiated with white light, indicating no change in respiration rate. Only slight changes in the rate of oxygen uptake were observed in the presence of the proton ionophore at the concentrations used, indicating a greater effect on photoresponse than on respiration.

In order to correlate the pH-dependent photoresponses described above and the mechanism of the *Stentor* photoreceptor, we closely examined the spectroscopic properties of the photoreceptor, particularly as a function of pH.

Healthy, living *Stentor* exhibits a fluorescence emission spectrum of the photoreceptor, which is much different from that of the dilute solubilized pigment complex. As seen in Fig. 6, the maximum is 660 nm, while the dilute pigment complex exhibits a maximum at 610 nm, and only a small shoulder at 660 nm. Since the emission of the liver cells was measured via front-surface emission (in a triangular cuvette), effects such as internal filtering and scattering, which could alter the shape of the spectrum, are minimized. The predomi-

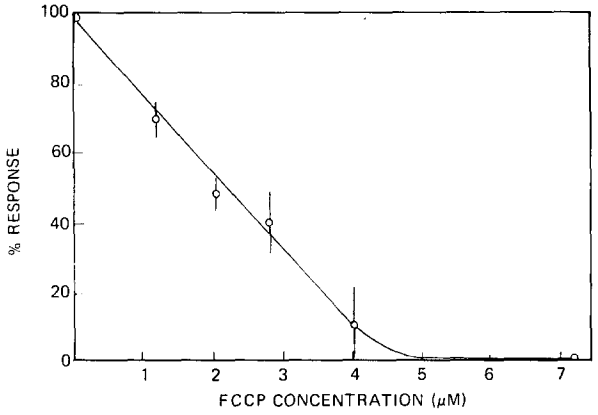

Fig. 5. Effect of FCCP on phototaxis of *Stentor coeruleus*. External pH was 7.8 in growth medium and FCCP (1.0 mg/ml in DMSO) was added in μl aliquots. When DMSO alone was added to the suspension in equal concentrations, there was no effect on response.

nant emission at 660 nm indicates the existence of some process in the excited state, which yields the 660 nm-emitting species, as the excitation spectra with respect to 610 and 660 nm emissions were identical. The efficiency of the process must be relatively high based on the relative intensity of the 660 nm and 610 nm emission peaks.

As mentioned, the dilute aqueous solution of photoreceptor ($A < 0.1$) exhibits a fluorescence maximum of 610 nm. If the concentration of the photoreceptor is increased, an increase in fluorescence intensity is observed as would be expected; however, the red-shifted emission begins to predominate, with a distinct isoemissive point at 622 nm (see Fig. 7).

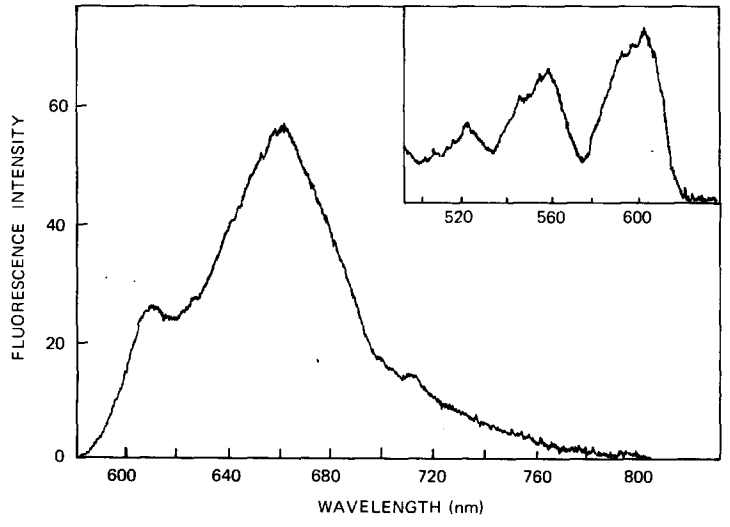

Fig. 6. Fluorescence emission spectrum of whole, living *Stentor coeruleus*, as measured by front surface excitation in a triangular cuvette. Excitation wavelength was 460 nm (5 nm excitation bandpass and 4 nm for emission). In addition, the emission was filtered for scattering by a Corning CS2-63 long pass filter.

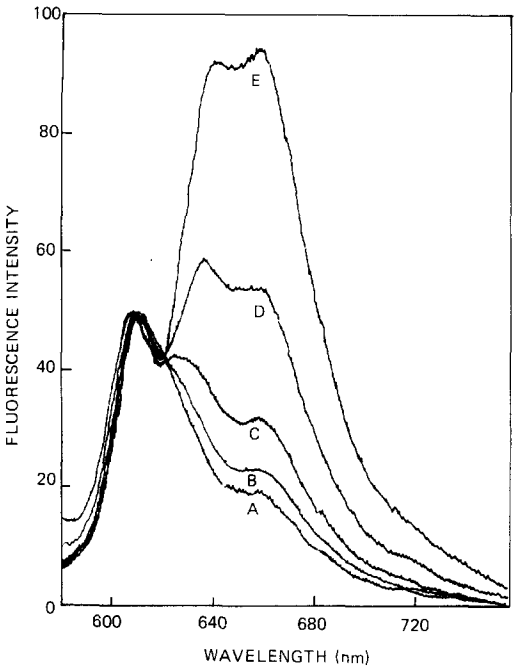

Fig. 7. Fluorescence emission spectra of *Stentor* photoreceptor in 0.01 M phosphate buffer at pH 7.4. The excitation wavelength was 560 nm (14 nm bandpass). The emission slit was varied between 6 and 7 nm to normalize intensity with respect to the 160 nm maximum. As the concentration of the photoreceptor was increased, the 660 nm maximum emerged. Absorbance at the excitation wavelength was used to monitor concentration; A, $2.0 \cdot 10^{-6}$ M; B, $4.7 \cdot 10^{-6}$ M; C, $9.5 \cdot 10^{-6}$ M; D, $1.9 \cdot 10^{-5}$ M; E, $2.9 \cdot 10^{-5}$ M.

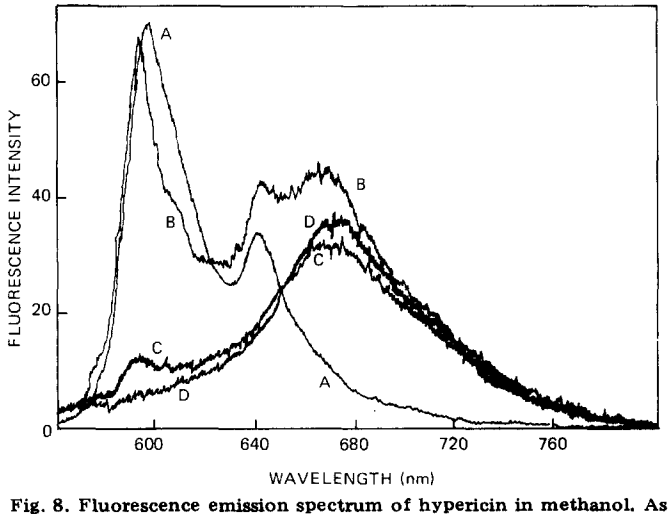

Fig. 8. Fluorescence emission spectrum of hypericin in methanol. As the solution is made basic by addition of NaOH, the red-shifted emission appears. The approximate concentration of NaOH for each curve: A, none; B, 0.1 M; C, 0.5 M; D, 1.0 M. Sensitivity of the instrument was ten times greater with curves B through D. Re-acidification of the solution with HCl yielded a curve identical to curve A, blue-shifted with its maximum at 583 nm, indicating the anionic form of the chromophore is fluorescing at 675 nm (λ_{ex} = 560 nm; hypericin concn. $1.1 \cdot 10^{-5}$ M).

The ratio of the intensity of 660 to 610 nm increases with increasing concentration, accompanied by a concomitant decrease in relative quantum yield across the entire emission spectrum, due in part to the lower ϕ_F of the red-shifted species.

Since the *Stentor* photoreceptor protein is also soluble in acetone [3], an identical set of experiments were conducted in acetone. In this case, no predominant emergence of the 660 nm band was noted. The ratio of I_{660nm}/I_{610nm} never exceed 0.7. In aqueous solution, the 660 nm emission is more than twice as intense as the 610 nm band. This indicates that the species responsible for the 660 nm emission is not found in acetone solution.

In all cases, the absorption maxima of the various concentrations were identical, indicating no formation of ground-state complexes. There was also no observed change in the fluorescence excitation spectrum, upon increasing concentration or moving the monitoring emission wavelength across the emission spectrum from 610 to 700 nm. This also indicates the species responsible for the 660 nm fluorescence of light is being formed in the excited state, not before absorption of light.

To test the possibility of excimer interactions, the viscosity of the aqueous solution was increased with sucrose from 0 to 900 cP and no change in either shape or intensity of the emission spectrum was noted. The CD spectrum also showed no change in shape or intensity over a 50-fold concentration range.

Hypericin, the chromophore of the *Stentor* photoreceptor pigment [3], does not give rise to a red-shifted emission, but addition of NaOH in methanol does give rise to an emission band at 667 nm, as seen in Fig. 8, which has a low quantum yield of approx. 0.0004.

The fluorescence spectrum of the *Stentor* photoreceptor at higher concentrations and the fluorescence maximum of living *Stentor* suggest that the predominant emitting species if the anionic form of the chromophore. Evidently, higher concentrations of the receptor complex in aqueous solution result in reconstitution of its native environment.

Fluorescence lifetimes were measured for both the live *Stentor* and the in vitro 'reconstituted' anionic fluorescence; for comparison, the lifetime of synthetic hypericin in basic methanol was also included in Table I. Heterogeneity in the four lifetimes is seen, indicating more than one fluorescing component. Analysis of the four lifetimes of each sample yields a short component (τ_1) in every case, with a lifetime of approximately 1.2 ns.

This short component of the observed lifetimes indicates that the lifetime of the anionic fluorescence is approx. 1.2 ns, and the excellent correlation of the short component in all samples lends further evidence to the formation of the anionic species in the excited state.

Although the fluorescence spectra of hypericin and the *Stentor* photoreceptor, either denatured or subjected to acetone, vary with pH, the fluorescence spectrum of the native photoreceptor is unaffected by pH. At first, this appears as a discrepancy in the postulated anionic fluorescence. This question will be discussed later, but apparently the chromophores of the photoreceptor complex are not exposed to the aqueous medium, since well known quenching agents such as KI, CsCl, and acrylamide, did not quench the fluorescence of the native photoreceptor.

TABLE I

FLUORESCENT LIFETIME ANALYSIS AT ROOM TEMPERATURE BY PHASE SHIFT (θ) AND BY MODULATION ($\cos\theta$) AT BOTH 30 MHz AND 10 MHz, EXCITING AT 560 nm

Sample [a]	τ_F 30 MHz		τ_F 10 MHz		Amplitude analysis [b]			
	By θ	By $\cos\theta$	By θ	By $\cos\theta$	τ_1	α_1	τ_2	α_2
1. Hypericin [c]	5.14 ± 0.2	5.24 ± 0.2	5.27 ± 0.2	5.30 ± 0.2	— [d]	—	4.98	0.93
2. Hypericin in 0.1 M NaOH	1.21 ± 0.1	1.97 ± 0.3	1.40 ± 0.2	2.37 ± 0.3	0.91	0.87	5.15	0.13
3. Photoreceptor complex $2 \cdot 10^{-6}$ M	2.67 ± 0.4	3.30 ± 0.4	3.01 ± 0.4	2.00 ± 0.4	1.31	0.45	4.55	0.55
4. Photoreceptor complex $2 \cdot 10^{-5}$ M	1.84 ± 0.3	2.32 ± 0.4	1.99 ± 0.3	2.56 ± 0.4	1.47	0.82	4.48	0.18
5. Live *Stentor*	1.42 ± 0.4	1.87 ± 0.5	1.54 ± 0.2	2.13 ± 0.3	1.21	0.90	4.95	0.10

[a] Solvents: 1 and 2, methanol; 3 and 4, 10 mM Trizma buffer, pH 7.4; 5, Growth medium, pH 7.8, with approx. 10^5 cells/ml in a triangular cuvette.
[b] τ_1 and τ_2: long and short lifetime components, respectively. α_1 and α_2: weighting components of respective lifetime components.
[c] From previously published data [3].
[d] Components which contributed less than 8% to the fluorescence lifetime were considered insignificant.

Fig. 9 shows a typical elution pattern of DMPC dispersion on a Sepharose 4B column. Fraction I was eluted with the void volume of the column, and fraction II was eluted as a broad peak. The relative amounts of fraction II depended on the sonication time, in agreement with work of Huang [10]. Fig. 9

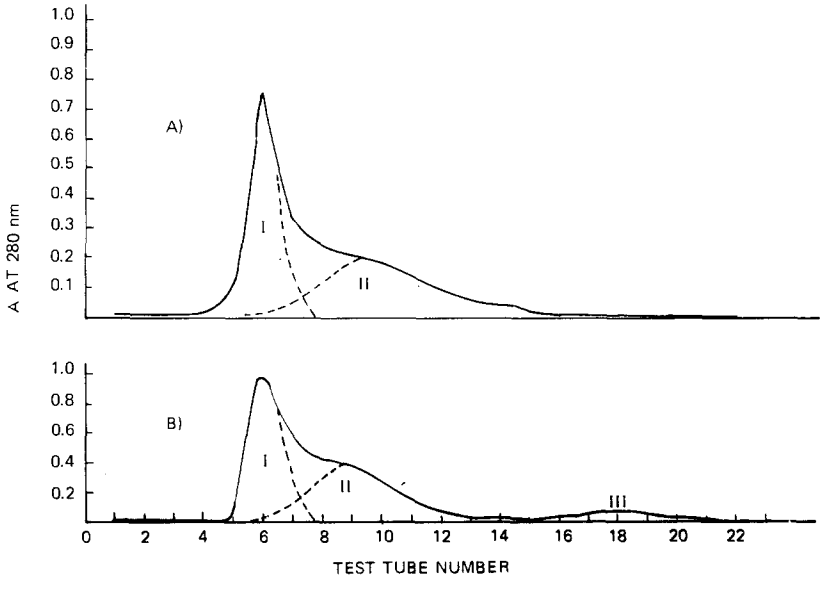

Fig. 9. Elution patterns of dimyristoyl phosphatidylcholine. (A) Dispersion of DMPC obtained from ultrasonication. DMPC dispersion (2 ml of 5% solution) was applied to a 2.5 × 20 cm lipid-treated Sepharose 4B column. (B) Sonicated mixture of DMPC and *Stentor* photoreceptor in (200 mM KCl + 1 mM EDTA) solution.

shows similar elution patterns of *Stentor* photoreceptor-entrapped DMPC on a Sepharose 4B column. The elution profiles were identical except for the fraction III peak in Fig. 9B. Fraction III exhibited the same elution volume as that of aqueous of acetone-extracted *Stentor* photoreceptor alone, indicating that fraction III is due to free *Stentor* photoreceptor. Fraction II was employed throughout these experiments.

In order to determine indirectly whether the *Stentor* photoreceptor was entrapped in the liposome or not, measurement of changes in fluorescence intensities of *Stentor* photoreceptor at 620 nm with 560 nm excitation wavelength was carried out with variation of temperature. As shown in Fig. 10, fraction II did not shown any phase transition temperature. Instead, *Stentor* photoreceptor-imbedded DMPC liposome showed the phase transition temperature at 23°C, which is in good agreement with that obtained by using parinaric acid-bound DMPC liposome [12]. Measurement of polarization vs. temperature showed the same result (data not shown). These results indicate that *Stentor* photoreceptor is definitely entrapped in the liposome.

Fluorescence changes of 9-aminoacridine in suspensions of live *Stentor* in growth medium solution were recorded during illumination. Fig. 11 shows the fluorescence quenching of 9-aminoacridine upon illumination of suspensions of live *Stentor*. When the light was turned off, the fluorescence increased slowly and resumed its original value. Such a slow return to the original level might be due to the slow diffusion of H^+ across the cell membrane, and the light-induced fluorescence quenching depends upon the fluence rate of actinic light (Fig. 12). These results indicate that intracellular pH of *Stentor* becomes lower than extracellular pH by a release of protons from the excited *Stentor* photoreceptor, implying the generation of a pH gradient.

On the other hand, very low concentration of nigericin (1.07 μmol/l) completely inhibited the light-induced fluorescence quenching of 9-aminoacridine.

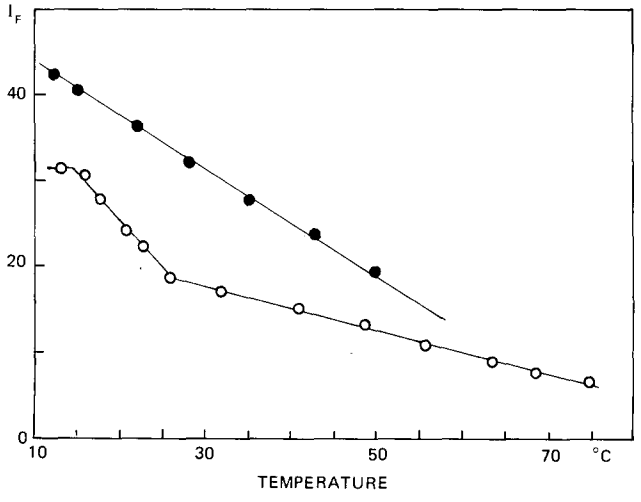

Fig. 10. Fluorescence intensity, I_F, of photoreceptor-DMPC liposomes vs. temperature. ○———○, photoreceptor-imbedded liposome; ●———●, photoreceptor-entrapped liposome. λ_{cm} 620 nm with λ_{ex} 560 nm.

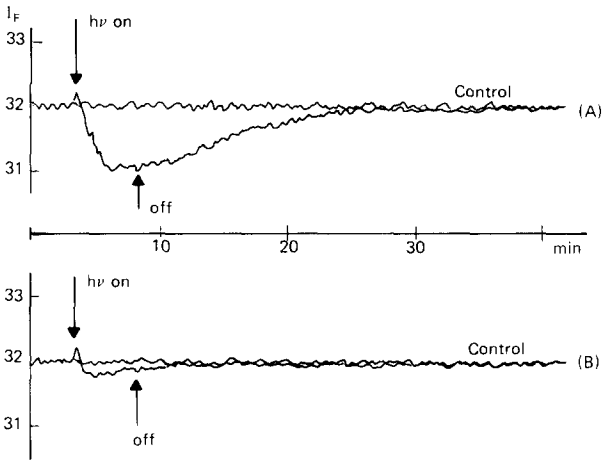

Fig. 11. (A) Light-induced fluorescence quenching of 9-aminoacridine in the suspension of live *Stentor* ($2 \cdot 10^3$ cells/2.5 ml). Initial pH 6.5. Final concentration of 9-aminoacridine was 4.0 μM. I_F was monitored at 450 nm with actinic wavelength between 575 and 750 with an American Optics mini lamp. (Filters used: CS2-63 and IR; light intensity: 100 W/m^2). (B) 1.07 μmol/l of nigericin in 2.5 ml suspension exhibited inhibition of I_F quenching. Controls (in dark) for both measurements are shown.

This result is matched with the observation that the same concentration of nigericin inhibited the photomovements of *Stentor* as shown in Fig. 13. These results strongly support the suggestion that photophobic behavior of the *Stentor* organism is triggered by proton movement across the cell membrane from the excited photoreceptor.

Similarly, photoreceptor-entrapped liposome was illuminated in the presence of 9-aminoacridine to see the light-induced pH change. Fig. 14 also shows a typical light-induced quenching of 9-aminoacridine in the photoreceptor-entrapped liposome in phosphate buffer, indicating that internal pH decreased upon illumination. It showed about 7% quenching, which corresponds to ΔpH

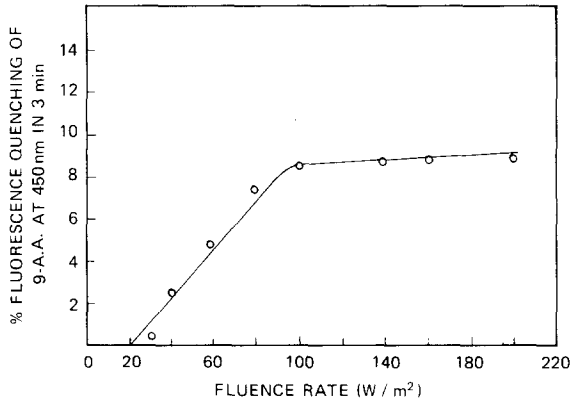

Fig. 12. Dose response of light-induced fluorescence quenching of 9-aminoacridine (9-A.A.) in suspensions of live *Stentor*. Actinic light intensity was controlled by using neutral density filters in addition to the cut-off and infra-red absorbing filters. Initial pH 6.5.

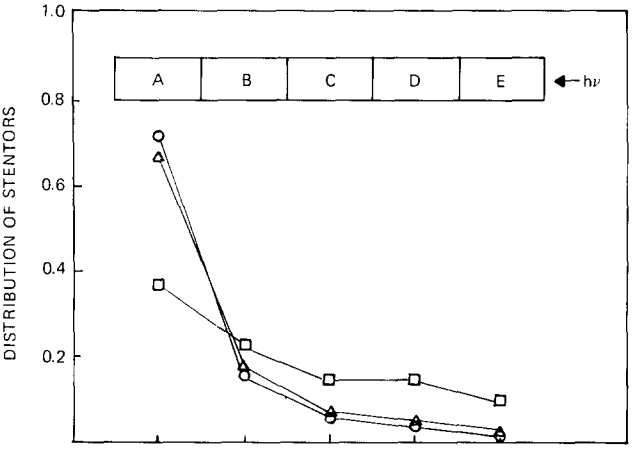

Fig. 13. Effect of nigericin on phototaxis of *Stentor*. 3 µl of nigericin stock solution ($1.51 \cdot 10^{-3}$ mol/l in DMSO) was added to 3.5 ml suspension of *Stentor*. For control 3 µl of pure DMSO were added to 3.5 ml suspension of *Stentor*. △———△, *Stentor* without DMSO and nigericin; ○———○, *Stentor* with DMSO; □———□, *Stentor* with nigericin. The data points represent fraction of *Stentor* cells in respective compartments, as shown.

= 0.8, indicating the ratio of moles of released H^+ to moles of photoreceptor is 0.26 on the basis of calculation, assuming a molar extinction coefficient at 605 nm of 50 000 and that the internal volume of liposome is smaller than the external volume by a factor of $3.5 \cdot 10^3$ [10]. The decreased fluorescence intensity returned to the original level when the light was turned off. It also showed fluence rate response as shown in Fig. 15. These results are similar to those of live *Stentor*, suggesting the possibility of vectorial orientation of the proton flux in the cell membrane.

It is interesting that the magnitude of light-induced fluorescence quenching of 9-aminoacridine in the photoreceptor-entrapped liposome changed with variation of medium pH, indicating that formation of the pH gradient across the bilayer is affected by medium pH (see Fig. 16). This result is similar to pH effect on phototaxis of live *Stentor*, as shown in Fig. 4.

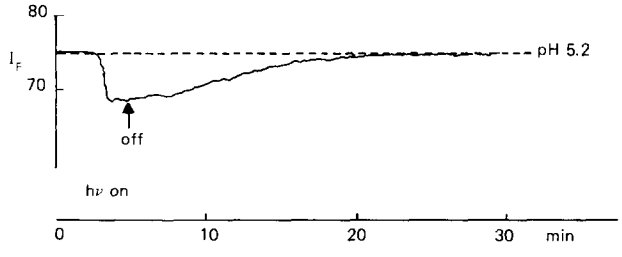

Fig. 14. Light-induced fluorescence quenching of 9-aminoacridine in photoreceptor-entrapped liposome. Medium solution, 10 mM posphate buffer; initial pH 5.8. Monitoring and irradiating methods are the same as in the legend for Fig. 11. Actinic light intensity was 200 W/m^2.

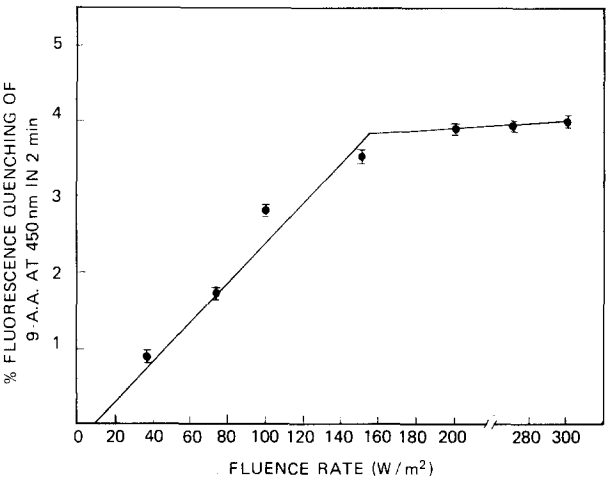

Fig. 15. Dose response of light-induced fluorescence quenching of 9-aminoacridine (9-A.A.) in photoreceptor-entrapped liposome. All methods are the same as in legend for Fig. 12. Initial pH 5.7. *A* at 605 nm = 1.0.

Discussion

As may be seen from the data, pH plays a critical role in the photoreceptive process in *Stentor coeruleus*. The pH dependence of photomovement indicates that external pH changes affect the cells' ability to sense the light. A number of possibilities exist to explain the drop in photoresponse below pH 6.

A critical pK_a involved in the photoresponse mechanism could be revealed

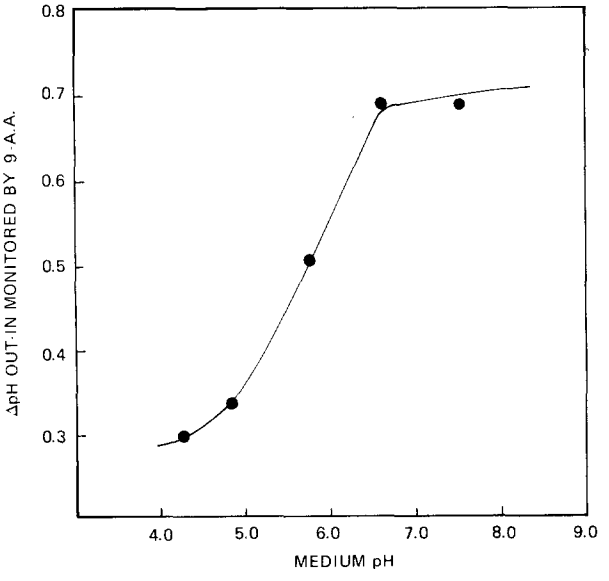

Fig. 16. External pH effect on light-induced fluorescence quenching of 9-aminoacridine (9-A.A.) in photoreceptor-entrapped liposome. Monitoring and irradiating methods are the same as in legend for Fig. 14.

by the lowering of external pH. Since the chromophore is not in direct contact with the aqueous solvent (demonstrated by attempts to quench fluorescence and insensitivity to pH in aqueous solution), it is difficult to say whether it is the pK_a of the chromophore which is responsible for inhibition or a subsequent residue in the sensory transduction mechanism. By virtue of its pK_a, histidine might be considered a candidate for the critical residue. Indeed, if the protein portion of the photoreceptor complex is responsible for conduction of protons away from the chromophore, histidine could function in this respect. Preliminary analysis of the associated protein confirms the presence of several histidine residues.

Subsequent disposition of the ejected protons could well affect existing membrane potentials by altering proton concentrations. Naturally, if the pH gradient across the cytoplasmic membrane is critical for the response, higher proton concentrations outside the cell might cause a neutralization of the pH gradient or a complete inversion of the gradient.

The basis for proton ionophore action lies with the ability of FCCP to quickly dissipate proton gradients across membranes, resulting in a loss of subsequent transduction processes. Since FCCP does have such a dramatic effect on photomovement, it may be assumed that pH gradients form the foundation of the photoresponse mechanism.

As a control in these experiments, oxygen consumption by *Stentor* was monitored in the presence of the ionophores, to insure any effects on photomovement were specific for this response only, and did not affect respiration rate. If, for example, the velocity of swimming increases in the light, one might expect a higher respiration rate and faster oxygen consumption. On the other hand, if ATP production is linked to a light-induced membrane potential, higher concentrations of ATP might retard respiration and cause a decrease in the rate of oxygen consumption. However, only a slight increase in the rate of oxygen consumption was observed, at 4 μM FCCP, while total inhibition of photomovement was seen.

Inhibition of phototaxis by nigericin was shown to be similar to inhibition of the light-induced proton gradient in *Stentor*. This result and the light-induced proton gradient in photoreceptor-entrapped liposomes, further clarify that a light-induced pH gradient is the primary triggering signal of *Stentor* photomovement.

If the red-shifted emission (Fig. 7) is due to the anionic species formed in the excited state, one would expect the shape of the spectrum to be affected by pH, as is the case with hypericin, where the chromophore is surrounded by water molecules. Standard quenching agents such as KI, CsCl, and acrylamide did not quench fluorescence of the chromophore in the photoreceptor complex, while free hypericin was quenched effectively by these reagents at similar concentrations.

Since the environment of receptor complex inhibits direct interaction of the chromophore with the aqueous solvent, changes in the pH of the buffered solution have no direct effect on the chromophore and the ratio of protonated and anionic species is dictated solely by the immediate environment of the receptor complex.

It may well be that the associated proteins serve to conduct the ejected

protons to the solvent. Higher concentrations of the photoreceptor complex results in reappearance of the anionic emission, indicating a partial reconstitution of the environment of the chromophore, favorable for deprotonation in the excited state. The nature of this environment is still unknown; however, a critical histidine residue might well be involved in transfering protons away from the chromophore in view of the pH-dependence of phototaxis and the 9-aminoacridine quenching in the model system. In vivo the protein might also serve to orient the chromophore properly in the granular membrane, so that subsequent disposition of the protons might yield membrane potentials required for photosensory transduction.

In view of the anionic fluorescence from living *Stentor*, it appears that the chromophore is losing one or more protons after absorption of light. The previously proposed mechanism of a lower pK_a in the excited state was contingent on the native pigment behaving in the same manner as the synthetic chromophore with respect to proton dissociation in the excited state [6]. Both the steady-state emission spectra and fluorescent lifetimes of the photoreceptor complex substantiate this mechanism and shed light on the efficiency of the process. Virtually all of the pigment molecules are protonated in the ground state since both absorption and fluorescence excitation spectra remained unchanged at higher concentrations. Once excited by light, however, they are rapidly and efficiently deprotonated during the short interval of time spent in the excited state. The ratio of fluorescent intensities of the two chromophore species in whole *Stentor* may be used to estimate the efficiency of the photoreceptive process. Since the only form absorbing light is the neutral (protonated) form, all anionic species are formed in the excited state and the ratio of anion to neutral chromophore ($[S^{-*}]/[SH^*]$) may be represented by

$$\frac{[S^{-*}]}{[SH^*]} = \frac{I_{660}}{I_{610}} \times \frac{\phi_{SH}}{\phi_{S^-}}$$

where ϕ is the quantum yield of fluorescence and I is the steady-state fluorescence intensity at the indicated wavelengths. When the fluorescence spectrum in Fig. 6 is resolved into the two fluorescing components, the resulting intensities indicate the ratio of $[S^{-*}]/[SH^*] \simeq 36$. The efficiency of deprotonation therefore exceeds 97%. This high efficiency explains the low-intensity threshold of 10% photoresponse attained with *Stentor* at only 0.1 W/m^2 (600 nm light).

Fig. 17 provides a schematic diagram of light absorption and subsequent deprotonation of the chromophore in the excited state. It is seen that anionic fluorescence predominates when the proton is efficiently removed from the chromophore in the excited state. To compete effectively with processes such as fluorescence, internal conversion and inter-system crossing, the rate constant for deprotonation must be extremely large, exceeding the diffusion controlled rate limit. Such a process would of necessity require assisting groups, such as proper amino acid residues, to allow the diffusion-controlled rate limit to be exceeded. A proton conduction network composed of one or more amino acid residues would not only allow a faster than diffusion-controlled rate, but could well serve to direct the released protons across its membrane. A picosecond spectroscopic measurement of the rise of the anionic fluorescence confirms

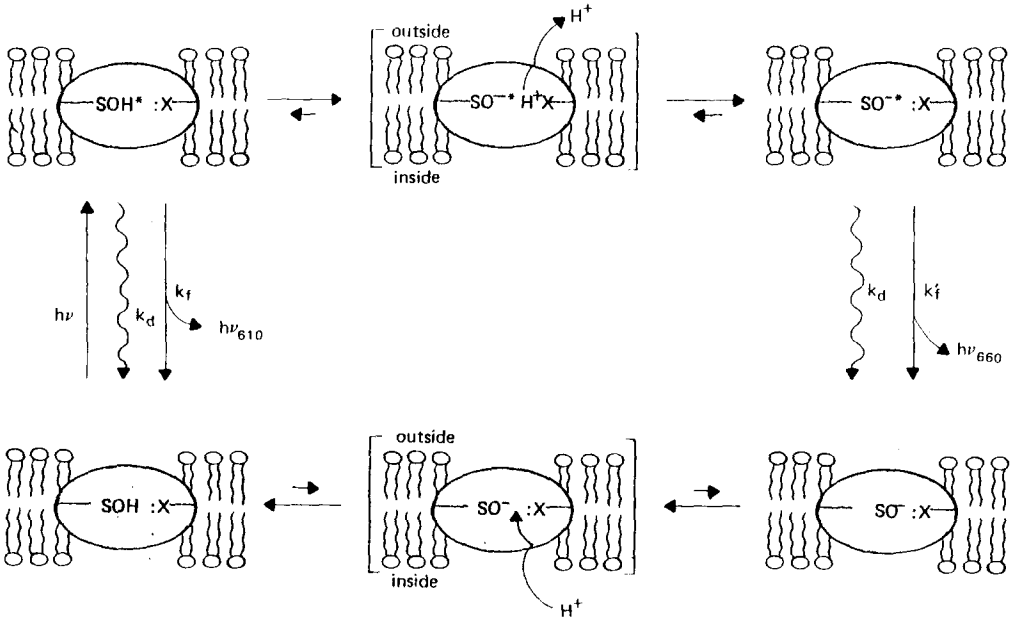

Fig. 17. Schematic diagram of the photoreceptor pigment (SOH) absorbing light and subsequent loss of a proton to an assisting base (:X⁻). This causes the equilibrium to shift towards the anionic form (SO^{-*}) in the excited state and thus, more anionic fluorescence is seen. k_f is the rate constant for fluorescence of each state and k_d represents the sum of the rate constants describing depopulating radiationless transitions.

that the proton dissociation in the photoreceptor complex (cf. Fig. 7) is at least two orders of magnitude faster than the diffusion-controlled rate (unpublished data).

The model system presented, of course, has no asymmetry as prepared. The fluorescence quenching of the 9-aminoacridine reflects a larger pH drop inside the liposome, due to the smaller internal volume.

Whether the photoreceptor complex is randomly distributed in the granular membrane in whole *Stentor* or if the photoreceptor complex is oriented and yields vectorial release of protons across the granular membrane is not yet known. The fact that the photoreceptor complex can generate proton gradients upon irradiation in a model system supports the proposed mechanism of the chromophore being a source of protons in its excited state.

The excellent correlation between pH-dependent phototaxis of the whole cells and the pH-dependent proton gradient formation in the liposome model system indicates the complex itself is responsible for the observed drop of response below pH 6. It is therefore conceivable that a critical protein residue is assisting in proton ejection by communicating the protons from the chromophore to the surrounding aqueous environment. The similarity of both the model and intact systems precludes the possibility of the pH affecting other gradients which might be involved in subsequent transduction. No pre-existing gradients are present in the liposome model system and the only effect of external pH change is to limit the ability of the photoreceptor complex itself from creating pH gradients at lower pH.

Conclusions

This work provides more evidence for the support of the previously proposed mechanism of photosensory perception in *Stentor*. Medium pH values below 5.5 abolish the *Stentor's* ability to sense the light, yet light perception is restored when the pH is returned to a value above 6. Both steady state fluorescence and fluorescence lifetimes of live *Stentor* and suspensions of the photoreceptor complex demonstrate that protons are being removed efficiently from the chromophore after absorption of light. When the photoreceptor complex is isolated and incorporated into artificial liposomes, pH gradients are formed upon irradiation with light. These gradients are abolished by FCCP, nigericin or lowering the pH, as is the photoresponse of *Stentor*. The photoreceptor complex is acting as a source of protons in the light to change resting proton concentrations across the granular membrane. This light-induced release of protons from the photoreceptor complex acts as the sensory signal for photomovement in *Stentor coeruleus*. Preliminary work indicates that the proton release induces Ca^{2+} influx (to be published).

References

1 Song, P.S., Häder, D.P. and Poff, K.L. (1980) Arch. Microbiol. 126, 181—186
2 Song, P.S., Häder, D.P. and Poff, K.L. (1980) Photochem. Photobiol. 32, 781—786
3 Walker, E.B., Lee, T.Y. and Song, P.S. (1979) Biochim. Biophys. Acta 587, 129—144
4 Newman, E. (1974) J. Protozool. 21, 729—737
5 Blumberg, S., Propst, S., Honjo, S., Otaka, T., Antanavage, J., Banerjee, S. and Margulis, L. (1973) Trans. Am. Microsc. Soc. 92, 557—569
6 Tartar, V. (1957) Exp. Cell Res. 13, 317—332
7 Wood, D.C. (1976) Photochem. Photobiol. 24, 261—266
8 Deamer, D.W., Prince, R.C. and Crofts, A.B. (1972) Biochim. Biophys. Acta 274, 323—335
9 Rouser, G., Kritchevsky, G., Heller, D. and Lieber, E. (1963) J. Am. Oil Chem. Soc. 40, 425—454
10 Huang, C.-A. (1969) Biochemistry 8, 344—351
11 Schuldiner, S., Rottenberg, H. and Avron, M. (1972) Eur. J. Biochem. 25, 64—70
12 Sklar, L.A., Hudson, B.S. and Simon, R.D. (1977) Biochemistry 16, 819—828